applied sciences

MDPI

Article

Hypromellose Acetate Succinates as a Single Mebeverine Hydrochloride Release-Modifying Excipient for Fused Deposition Modeling

Mateusz Kurek [1,*], Margarida Berardo Lopes Nunes [2], Witold Jamróz [1], Justyna Knapik-Kowalczuk [3], Marian Paluch [3] and Aleksander Mendyk [1]

[1] Chair of Pharmaceutical Technology and Biopharmaceutics, Faculty of Pharmacy, Jagiellonian University Medical College, Medyczna 9, 30-688 Kraków, Poland; witold.jamroz@uj.edu.pl (W.J.); aleksander.mendyk@uj.edu.pl (A.M.)
[2] Faculdade de Farmácia, Universidade de Lisboa, Av. Prof. Gama Pinto, 1649-003 Lisboa, Portugal; margaridaberardolopes@gmail.com
[3] Institute of Physics, Faculty of Science and Technology, University of Silesia in Katowice, 75 Pułku Piechoty 1a, 41-500 Chorzów, Poland; justyna.knapik-kowalczuk@us.edu.pl (J.K.-K.); marian.paluch@us.edu.pl (M.P.)
* Correspondence: mateusz.kurek@uj.edu.pl

Abstract

Background: Three-dimensional (3D) printing has been established in pharmaceutical sciences for preparing customized dosage forms with intricate release profiles. However, realizing this potential requires complex design strategies and the careful use of various excipients. This study was designed to evaluate the utility of hypromellose acetate succinate (HPMC-AS) as a singular release-modifying excipient for manufacturing oral solid dosage forms via fused deposition modeling (FDM) 3D printing. Methods: The scope of work encompassed comprehensive material characterization, formulation and production of drug-loaded filaments using hot-melt extrusion (HME), subsequent FDM 3D printing of tablet geometries, and in vitro dissolution studies using mebeverine hydrochloride (MebH) as the model drug. Results: Initial HME processing indicated that the HPMC-AS-based filaments were brittle, presenting technical challenges for direct 3D printing. This issue was successfully overcome by incorporating an additional preheating stage into the FDM printing process, which enabled production of the tablets. Dissolution analysis demonstrated that the 3D-printed mebeverine hydrochloride tablets exhibited delayed and sustained-release characteristics. Conclusions: These results confirm the viability of HPMC-AS as a standalone functional excipient in FDM 3D printing to produce tailored, complex drug delivery systems.

Keywords: hypromellose acetate succinate; mebeverine hydrochloride; modified release; 3D printing; hot-melt extrusion

Check for updates

Academic Editor: Jason G. Parsons

Received: 30 December 2025
Revised: 14 January 2026
Accepted: 21 January 2026
Published: 26 January 2026

Copyright: © 2026 by the authors. Licensee MDPI, Basel, Switzerland. This article is an open access article distributed under the terms and conditions of the Creative Commons Attribution (CC BY) license.

1. Introduction

Over the last years, various additive manufacturing methods, more commonly known as three-dimensional (3D) printing, have been introduced into the field of pharmaceutical sciences [1]. Among these methods, fused deposition modeling (FDM) has demonstrated significant potential for preparing dosage forms [2]. Numerous studies conducted by various research groups have demonstrated the applicability of FDM for producing a wide range of dosage forms. This, among others, includes orodispersible films (ODFs),

tablets (ODTs), immediate-release and sustained-release tablets, microneedles, and implants [3–6]. Creating a successful 3D-printed dosage form with specific properties begins with preparing a drug-loaded filament. This filament is a uniform, rod-shaped extrudate typically produced using hot-melt extrusion (HME). In this process, an active pharmaceutical ingredient (API) is homogenized with a polymer in a twin-screw extruder and then pushed through a circular die, usually 1.75 mm in diameter. The resulting filament must have sufficient mechanical strength to withstand the forces in the 3D printer's printhead. Furthermore, it is crucial that the filament's diameter is uniform, as this directly affects the reproducibility of the printed drug mass and dose [7,8]. The development of filament extrusion and its characterization methods have not kept pace with the rapid advancement of FDM 3D printing. Most published research concentrates on the 3D printing process and the properties of the final dosage forms. Consequently, there is often a lack of detailed information regarding filament preparation, evaluation methods, and quality attributes. This is a significant gap, as the composition of the polymer matrix and the quality of the filament itself have a profound influence on the properties of the final dosage form [9].

Selecting the right excipients is one of the most crucial steps in developing a dosage form. For 3D-printed dosage forms, the polymer is the primary excipient, and its properties significantly impact both the filament and the final product. While a few pharmaceutical-grade polymers can be used alone for filament production—such as poly(vinyl alcohol), hypromellose, and Kollicoat® IR—most require the addition of other functional excipients. These can include plasticizers, disintegrants, flow enhancers, or stabilizers. One polymer that could expand the applications of 3D printing is hypromellose acetate succinate (HPMC-AS). However, it is rarely used as a standalone material due to its rigidity and temperature sensitivity [10,11]. For example, Goyanes et al. used 5 or 15% of methylparaben as a plasticizer in their paracetamol-loaded HPMC-AS-based filaments, and Shojaie et al. utilized triethyl citrate or sorbitol for the same reason. Both research groups also used magnesium stearate or colloidal silica as lubricants [12,13]. Despite these challenges, its pH-dependent solubility makes it an excellent candidate for creating delayed and sustained-release tablets.

Mebeverine hydrochloride is a freely water-soluble antispasmodic used in the treatment of spasm-associated abdominal pain, especially in the treatment of irritable bowel syndrome and other gastrointestinal conditions. It is usually formulated in the form of tablets or capsules also with modified release. As its therapeutic effect is mainly local, it has to be delivered to the site of action, which is usually the large intestine [14].

This study aimed to evaluate how different grades of hypromellose acetate succinate could be used to modify the release of a highly water-soluble model drug, mebeverine hydrochloride, from tablets produced via fused deposition modeling. The primary objective of this research was to investigate the possibility of using HPMC-AS as an auxiliary substance that does not require the use of any functional additives at the printing stage, which has not been studied to date. The research also included a comprehensive characterization of hot-melt extrusion and 3D-printing processes, as well as of the raw materials and resulting filaments, focusing on their thermostability and mechanical properties. Furthermore, we developed and utilized new jigs specifically for testing the filament's breaking resistance.

2. Materials and Methods

2.1. Materials

Mebeverine hydrochloride (abbreviated as: MebH, 4-[ethyl-[1-(4-methoxyphenyl) propan-2-yl]amino]butyl 3,4-dimethoxybenzoate; hydrochloride, MOEHS, Lessines, Belgium) was used as the model active substance. Poly(vinyl alcohol) (PVA, Parteck® MXP 4-88, M_W = 32,000 g/mol, hydrolysis degree 85–89%, Merck®-KGaA, Darmstadt, Germany) and three medium particle size grades of hydroxypropylmethylcellulose acetate succinates (HPMC-

AS), namely, AQOAT® AS-LMP, AQOAT® AS-MMP, and AQOAT® AS-HMP—kindly donated by SE Tylose GmbH & Co., KG (Wiesbaden, Germany)—were used as a matrix-forming polymer for the preparation of the filaments and 3D-printed tablets. Hydrochloric acid solution and trisodium phosphate dodecahydrate (both from Merck® KGaA, Darmstadt, Germany) were used in the dissolution media. The water used in all experiments was produced by the Elix 15UV Essential reverse osmosis system (Millipore SAS, Molsheim, France).

2.2. Raw Materials and Powder Blends Characterization

2.2.1. Particle Size Measurement

The measurements of particle size distribution were performed using a Mastersizer 3000 equipped with an AeroS unit (Malvern Instruments, Malvern, UK) in a dry dispersion method. The sample was placed in an AeroS unit hopper and fed to the venturi dispenser until the obscuration reached the given value (between 0.5 and 6%), and then the measurement was carried out automatically. The relationship between the particle size and light intensity distribution pattern was found based on the Fraunhofer diffraction theory. The reported data represents the averages from six series (n = 6) of measurements of each sample and the distribution span.

2.2.2. Flowability

The flowability of powders was determined by measuring the angle of repose, according to the Ph. Eur. monograph 2.9.36 [15]. Powder was poured into a sieve container, positioned above a 60 mm diameter flat, round surface, allowing the powder to form a conical pile. A measuring rod with an attached angle and metric scale was used to determine the angle of the cone's slope relative to the horizontal surface. This maximum angle represents the angle of repose. The measurement was repeated three times (n = 3), and the average value was calculated.

2.2.3. Wettability

The wettability of the substances was assessed using the sessile drop technique with a DSA25 drop shape analyzer (Krüss, Hamburg, Germany). Compacts, prepared from the substances using an Atlas™ manual 15-ton hydraulic press (Specac, Kent, UK), served as the sample. A 2 µL drop of distilled water, generated by an automated syringe, was deposited onto each tablet surface. To minimize the influence of water penetration into the compressed powder, the contact angle was measured immediately after drop deposition. Each sample underwent six contact angle measurements (n = 6), and the average value was calculated.

2.2.4. Thermogravimetric Analysis

The thermal stability of each formulation component (active substance and polymers) with respect to mass loss was evaluated using a TG50 thermogravimetric analyzer coupled with an MT5 balance (Mettler-Toledo, Greifensee, Switzerland). Samples, contained in 100 µL aluminum TGA crucibles, were heated from 30 °C to 450 °C at a 10 °C/min rate under a 50 mL/min nitrogen purge. Sample degradation was quantified by the percentage weight loss observed throughout the tested temperature range.

2.3. Hot-Melt Extrusion

Filaments were extruded using a 12 mm, 40D corotating, twin-screw extruder (RES-2P/12A Explorer, Zamak Mercator, Skawina, Poland) with our standard screws with three kneading zones. The specific screw configuration was described in our previous work [16]. The setup also included a gravimetric feeder (MCPOWDER® Movacolor®, Sneek, The Netherlands), an air-cooled conveyor belt (Zamak Mercator, Skawina, Poland), and a

two-dimensional laser diameter gauge (LDM25XY, Mercury-Tech Co., Ltd., Zhengzhou, China) to monitor the filament diameter on-line. For each batch, a 100 g mixture was prepared, with mebeverine HCL making up 40% of the total weight. The mixture was then extruded through a 1.75 mm die. The screw speed was maintained at 100 rpm. To optimize the process for each mixture, the temperature profile was adjusted based on the thermal properties of the materials. The entire process was monitored by tracking key parameters like torque, die pressure, motor loads, and the temperature of each heating zone.

2.4. Filament Characterization

The filaments were characterized in terms of API content and diameter uniformity as well as mechanical properties such as elasticity, tensile strength, and resistance to bending and crushing.

2.4.1. Drug Content Uniformity

Ten randomly selected pieces of each extrudate (n = 10) were accurately weighed to determine API content. The samples were placed in conical flasks filled with 50 mL phosphate buffer, stirred at 37 °C for 24 h in a Memmert® water bath (WNB 22, Schwabach, Germany), and filtered through CHROMAFIL® Xtra CA45/25 syringe filters. The concentration of mebeverine hydrochloride was determined spectrophotometrically at 292 nm using a Shimadzu UV1900 spectrophotometer (Kyoto, Japan). The specificity of the analytical method was checked, and linearity (R^2 = 0.9996) was confirmed in the range from 10 to 120 µg/mL.

2.4.2. Filament Diameter Uniformity

The filament diameter was controlled in-line using a two-dimensional laser gauge (LDM25XY, Mercury-Tech Co., Ltd., Zhengzhou, China) to optimize the extrusion process. Additionally, the filaments' diameter uniformity was evaluated off-line using a Mitutoyo micrometer screw (Kawasaki, Tokyo, Japan). This involved taking 20 subsequent diameter measurements every 10 cm and calculating their average.

2.4.3. Mechanical Properties

To evaluate the mechanical properties, stretching, three-point bending, and crushing tests were performed using an EZ-SX texture analyzer (Shimadzu®, Kyoto, Japan) with specially designed adapters to standard texture analyzer grips (Figure 1).

For the stretching test, six filament samples (n = 6) were randomly selected from each formulation. Each sample had a total length of 130 mm, with a 100 mm section designated for measurement. After selection and diameter assessment, the filaments were secured in the grips of a tensile tester and stretched with 1000 mm/min speed until they ruptured. This process allowed for the determination of the tensile strength and Young's modules of the filaments.

In three-point bending tests, six filament samples were randomly selected from each formulation. Each sample was positioned horizontally on supporting pins spaced 50 mm apart. An indenter was then lowered at a 20 mm/min speed to bend the filament at its midpoint, directly between the two supports. The maximum bending force and corresponding displacement were recorded.

For the crushing strength test, we manufactured specially designed jigs. The crushing components were gear rolls sourced from a 3D printer printhead. Each filament sample was positioned horizontally on a support, with one gear roll underneath. The second gear roll was lowered at a 20 mm/min speed and applied force to the filament until it was crushed. We recorded the maximum force required to crush the filament.

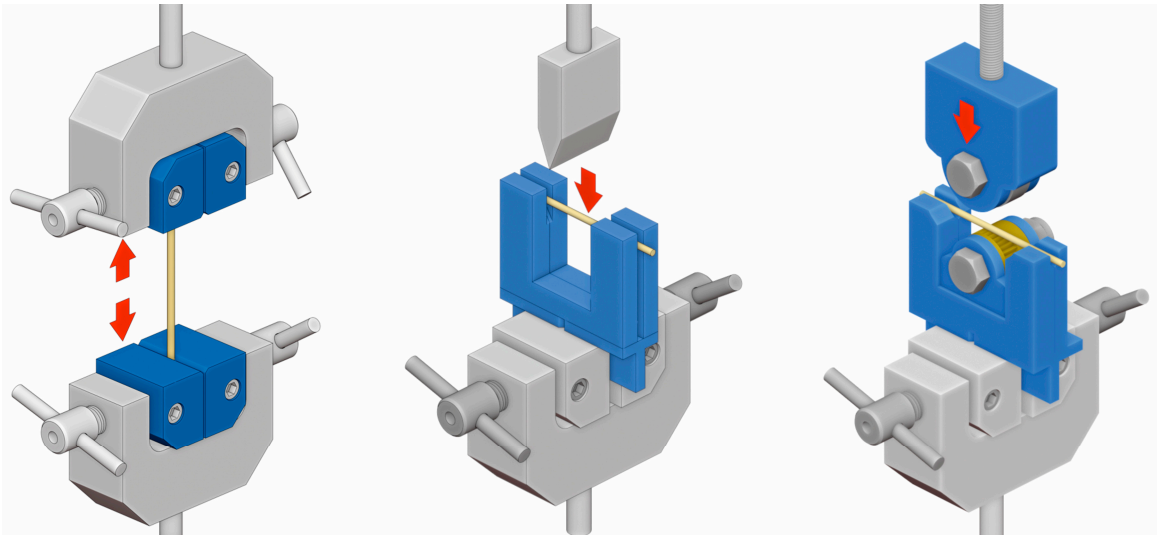


Figure 1. The design of the filament testing grips for texture analyzer. Blue parts were designed and printed out especially for pharmaceutical filament testing, red arrows represent the movement direction of the grips.

2.4.4. Differential Scanning Calorimetry

The thermal properties of mebeverine hydrochloride and all investigated MebH-based binary systems were measured using the Metler Tolledo STARe system (Columbus, OH, USA), equipped with an HSS8 ceramic sensor, 120 thermocouples, and the liquid nitrogen cooling accessory. The measuring device was calibrated for temperature and enthalpy using zinc and indium standards. The samples were placed in an aluminum crucible (40 µL). Both the initial, raw crystalline MebH and the pulverized 3D-printed tablets were heated up from 25 °C to 180 °C with a 10 °C/min rate under constant 50 mL/min nitrogen flow. The glass transition temperature was determined as the midpoint of the glass transition step, while the crystallization and melting temperatures were established at the onsets of the exothermic and endothermic peaks, respectively.

2.5. Three-Dimensional Printing

The design of the tablets was an oblong shape of 20 mm in length and 10 mm in width with 100% rectangular infill. The tablets were printed by an FDM ZMorph 2.0 S 3D printer (Wroclaw, Poland) equipped with a 1.75 mm commercially available printhead with a 0.3 mm nozzle. The raster angle was 0° and the deposition angle was equal to 90°. All tablets were printed with the same printing speed, equal to 10 mm/s. The melted filaments were deposited by the printing toolhead onto the printing table covered by the COROPad™ adhesive pad (HMF Chemicals, Grodzisk Mazowiecki, Poland) warmed up to 65 °C. The printing temperature was set to 175 °C. The differences between the actual and theoretical diameters of the filaments were compensated by changing the filament diameter settings in the slicing software (Voxelizer 1.4.18, Wroclaw, Poland). All tablets were weighed immediately after printing. Due to the low mechanical resilience of the AQOAT filaments, warm air stream preheating the filament above the printhead was utilized to prevent filament crushing.

2.6. Dissolution Studies

Dissolution studies were performed using a Vision G2 Elite 8 dissolution bath (Teledyne Hanson Research, Chatsworth, CA, USA). The tests were performed on six tablets (n = 6) from each batch. The temperature was maintained at 37 ± 0.5 °C, and the paddle speed was set to 50 rpm. The two-phase dissolution with a total time of 24 h was performed;

the initial release of MebH was carried out in a 750 mL 0.1 mol/L HCl solution at pH = 1.2 for 2 h, followed by a buffer stage at pH = 6.8 for 22 h. The pH change was made by the addition of 250 mL of 0.20 mol/L solution of trisodium phosphate dodecahydrate. Samples were taken every 0.5 h and analyzed spectrophotometrically on-line with a Shimadzu UV1800 spectrophotometer (Kyoto, Japan) equipped with an 8-position cuvette changer and flow-through cuvettes. The samples were analyzed at λ = 292 nm. The results represent averages with their corresponding standard deviations (SD).

3. Results and Discussion

The research was divided into a few stages—namely, preformulation, technological, and analytical studies. Poly(vinyl alcohol) (Parteck® MXP 4-88) was used as a reference polymer in this study as it was proven in many studies that it is possible to achieve good quality filaments with this excipient and it can sustain release of the API due to its swelling properties [4].

At the first stage of the research, preformulation studies were performed to assess the technological attributes of mebeverine hydrochloride and the used excipients. The results of laser diffraction analyses showed differences between the API and polymers particle size distributions (Figure 2). Median particle size (Dv50) of MebH was 10.8 ± 0.25 µm, while polymers were characterized by much bigger median particle size and were 57.3 ± 0.77 µm, 298 ± 8.44 µm, ±9.23 µm, and 259 ± 5.3 µm for PVA, AQOAT AS-LMP, AQOAT AS-MMP, and AQOAT AS-HMP, respectively. From a technological point of view, this difference may result in particle segregation and possible inhomogeneity in the polymer matrix. On the other hand, big AQOAT particles promote better flowability of the final blend and, thus, better filament diameter uniformity. The AQOAT particle size distributions revealed that AQOAT AS-HMP had the highest share of small particles, as the value of 10th percentile of particle size distribution (Dv10) was approximately 2-fold smaller than for the remaining two HPMC-AS grades. It is also clearly visible in Figure 2 where particle size distributions are shown. The dark red plot for AQOAT AS-HMP has a tail at the small particles side, which resulted in a worse flowability of the polymer and final blend.

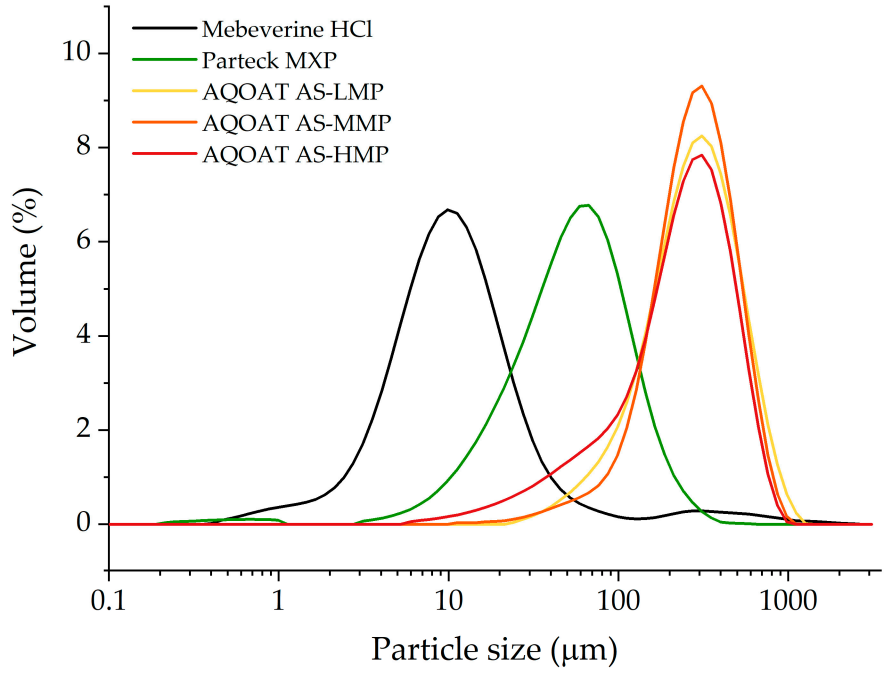


Figure 2. Particle size distributions for API and polymers.

The flow properties of the API and excipients were also assessed, as they impact the process robustness. The results of the angle of repose measurement are given in Table 1. According to the Eur. Ph., Mebeverine hydrochloride is characterized as a very, very poor flowing powder, which may be an issue in the process of feeding the material to the extruder barrel. The polymers were also of limited flowability, but the final blends were uniformly fed to the extruder by the gravimetric feeder, and filaments of uniform diameter were achievable.

Table 1. Properties of API and polymers.

Substance	Wettability (°)	Loss on Drying (%)	Angle of Repose (°)	Flow Property
MebH	42.9 ± 6.6	0.17	>66	Very, very poor
Parteck MXP	72.8 ± 8.4	2.36	40	Fair
AQOAT AS-LMP	68.6 ± 3.5	2.49	39	Fair
AQOAT AS-MMP	72.2 ± 6.1	2.32	36	Fair
AQOAT AS-HMP	71.80 ± 4.18	1.80	42	Passable

The contact angle measurements were performed in order to evaluate the effect of wettability of matrix-forming polymer on the dissolution of MebH. All polymers were characterized by comparable wettability expressed as contact angles around 70° while API was better wettable as its contact angle was much lower, ca. 43°. Thermogravimetric analysis allowed us to check whether API or polymers will be thermostable enough to withstand high processing temperatures, as hot-melt extrusion and fused deposition modeling use elevated temperatures. In Figure 3 the TGA curves are presented, and the actual temperatures which were utilized during the filament extrusion and three-dimensional printing processes are marked with dashed and dotted lines, respectively. The TGA thermograms of the polymers displayed an initial mass loss of roughly 1.8–2.5% between 30 °C and 100 °C, attributed to the evaporation of adsorbed water and residual moisture from the sample surface. The variations in moisture content are directly correlated with the ratio of acetyl to succinyl groups in various grades of HPMC-AS. AQOAT AS-HMP is distinguished by the largest concentration of acetyl groups, which enhances hydrophobicity and, thus, leads to reduced moisture content. It is clearly visible that both processes were conducted in the "safe zone". The 3D printing process required higher temperatures, as the molten material is pushed through the smaller nozzle and proper rheological properties of the material have to be assured.

The filament extrusion processes went smoothly and repeatedly. The process parameters for the extrusion of HPMC-AS-based filaments were maintained the same to compare the outputs of the process while PVA-based formulation was extruded with previously optimized parameters unrelated to AQOAT-based formulations. As can be seen from Table 2, at the same process conditions the differences in extrusion process are almost negligible; however, it is worth noting that the throughput of the extrusion process measured as a linear speed of filament production was considerably lower for the AQOAT AS-HMP-based filament. This may be attributed to its higher fraction of small particles and worse flowing properties, which resulted in slower feeding rates. Despite poor flowability of API/polymer mixtures the feeding consistency was good enough to achieve filaments with uniform diameter. The dimension deviations were kept below ±50 µm for all AQOAT-based filaments and were only slightly higher for filaments made with Parteck MXP. The filament diameter

uniformity is even more important than the diameter itself, as it can be corrected in the 3D printer software; but, the consistent material (filament) feeding to the printhead is of crucial importance for the final dosage form weight and, thus, dose uniformity. The torque and the die pressure were the highest for the AQOAT AS-LMP-based formulation; however, they are still acceptable and far from the limits.

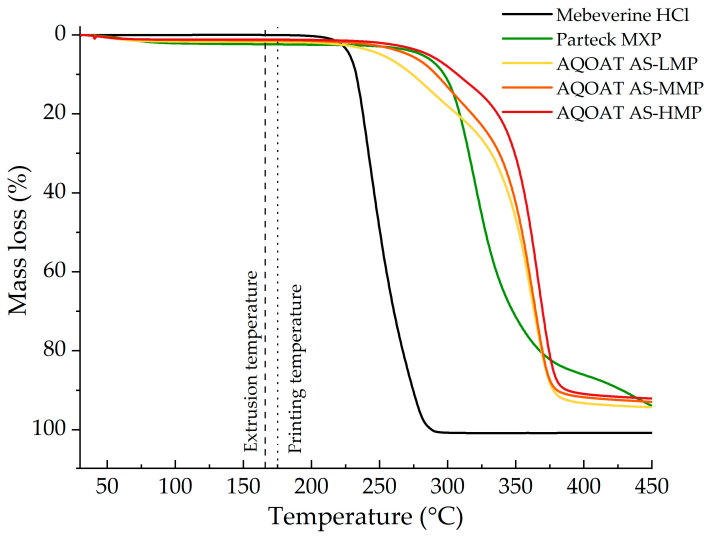


Figure 3. Mebeverine hydrochloride and polymers TGA curves. An insert represents magnification of the region of interest.

Table 2. Extrusion process outputs.

Formulation	Torque (Nm) ± SD	Die Pressure (Bar) ± SD	Throughput (m/min) ± SD	Filament Dia. (mm) ± SD
PVA + MebH	1.78 ± 0.17	8.05 ± 1.25	0.81 ± 0.121	1.77 ± 0.057
A-LMP + MebH	3.19 ± 0.16	33.38 ± 1.78	1.05 ± 0.119	1.70 + 0.025
A-MMP + MebH	2.78 ± 0.09	26.50 ± 0.92	1.06 ± 0.002	1.72 ± 0.044
A-HMP + MebH	2.80 ± 0.07	25.19 ± 2.07	0.93 ± 0.035	1.74 ± 0.026

One of the most important properties of the filament is its mechanical resilience. As it is subjected to forces in the printhead of the 3D printer, it must be durable enough to withstand these forces. If the filament is too weak it will bend or crush in the printhead and block it [17]. To evaluate these, three different mechanical tests were conducted, namely a stretching, a three-point bending, and a crushing test. As mentioned before, PVA-based filaments were made as a reference; thus, the results obtained for AQOAT-based filaments are compared to the PVA-based one. Young modulus (YM) is the measure of elasticity and stiffness of the filament, and it is determined in the stretching test, the higher the YM value the lower the elasticity of the filament. From the values presented in Table 3, it can be concluded that the filaments were of comparable elasticity, as the average values of the Young modulus are comparable. However, the printability of the filaments was different. PVA-based filaments possessed mechanical properties sufficient to the 3D printing process while all AQOAT-based filaments were hardly printable; in fact, a modification of the 3D printing process consisting of preheating of the filament just above the printhead using a blow of hot air had to be performed. Without this, the filaments were crushed between the gear rolls of the printhead. Because the stretching test did not differentiate the filament in terms of printability, two additional tests were performed: three-point bending test and

crushing test. The forces exerted on the filament during three-point bending and crushing tests act perpendicular to the material's long axis, whereas tensile tests apply stretching forces along the long axis; thus, the results are not directly comparable. Moreover, in a three-point bending test, the upper surface experiences maximum compression, while the lower surface undergoes maximum tension. We designed and printed a special adapter to test the crushing resistance between two gear rolls taken directly from the 3D printer, which are used to feed the printhead with the filament and where filament rupture usually occurs. Both tests differentiated AQOAT filaments from PVA filaments. In the crushing test, the filament made from PVA was not crushed and the upper limit of the applied force, i.e., 500 N, was reached while HPMC-AS-based filaments were broken between 68.8 and 77.6 N of the applied force. The weakest filament was made from AQOAT AS-LMP. This filament was also characterized by the lowest resistance to bending, as the strain was the lowest, i.e., 0.77 mm, and it was caused by a force of 4.42 N. Other AQOAT-based filaments were slightly more durable but not enough to withstand the forces in the printhead without preheating. The slight differences in the mechanical properties of the filaments made from different AQOAT grades may be attributed to the degree of substitution with acetyl groups. A higher degree of acetylation can lead to improved mechanical properties, while low acetyl substitution can cause reduced mechanical resilience and higher brittleness, which was observed in AQOAT AS-LMP-based filaments [18].

Table 3. Filament mechanical properties attributes.

Formulation	Stretching	Crushing	Three-Point Bending	
	Young Modulus (N/mm^2) ± SD	**Force Max. (N) ± SD**	**Force Max. (N) ± SD**	**Bending Depth (mm) ± SD**
PVA + MebH	2075.7 ± 58.20	>500	N/A	∞
A-LMP + MebH	2121.8 ± 83.60	68.8 ± 7.1	4.42 ± 0.38	0.77 ± 0.09
A-MMP + MebH	1986.9 ± 105.5	77.1 ± 14.9	5.02 ± 0.38	0.93 ± 0.11
A-HMP + MebH	1947.8 ± 174.2	77.6 ± 11.5	4.87 ± 0.32	0.81 ± 0.07

Above the glass transition temperature (T_g), the material properties change dramatically. Below the T_g, the material is brittle and hard. Instead of undergoing deformation, it usually breaks, while above T_g it becomes more plastic and elastic—what prevents crushing [19]. We have performed a differential scanning calorimetry measurement to check whether we are able to improve printability by simply heating up the filaments (Figure 4). As the values of glass transition temperature for AQOAT-based formulation were 40 °C, 41 °C, and 43 °C for AQOAT AS-LMP, AS-MMP, and AS-HMP, respectively, we were able to preheat the filaments above T_g by using hot air blow just above the filament entering the printhead. The preheating process utilized a standard hair dryer with an airflow velocity of 7.1 to 7.3 m/s, positioned around 15 cm from the filament, resulting in a filament temperature exceeding 43 °C. The procedure was observed utilizing a Thermal Imaging Camera FLIR E5. This simple procedure allowed us to print tablets without any plasticizers and to obtain information about the impact of the pure polymer to dissolution of mebeverine hydrochloride.

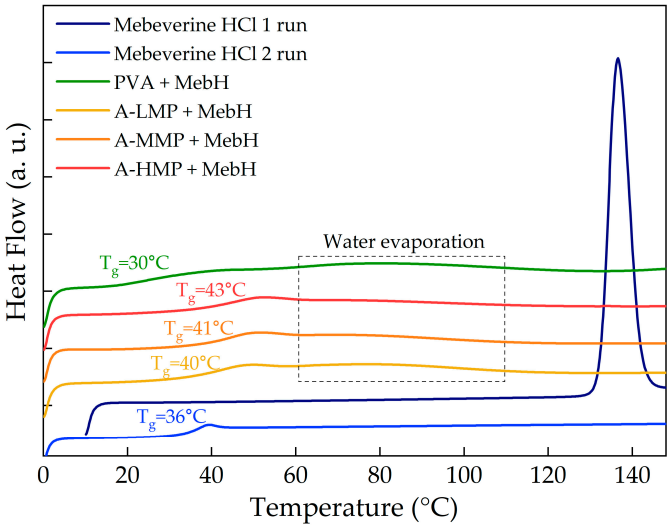


Figure 4. DSC thermograms for neat mebeverine hydrochloride and powdered filaments.

The tablet design, specifically the number of layers, was modified to attain a strength of 100 mg across all formulations. The tablets were printed with 100% infill to assess their maximum release sustaining capability, as any loosening of the structure increases the available surface area and accelerates dissolution. The mebeverine hydrochloride release profiles were evaluated in a two-stage dissolution experiment. The dissolution profiles are presented in Figure 5 and raw data is gathered in Table S1 in the Supplementary Materials. The gastric phase was conducted in the hydrochloride acid solution in pH = 1.2 for two hours and then pH was changed to 6.8; the dissolution test continued until a total run time of 24 h was reached. As the AQOATs are characterized by pH-dependent solubility only a small amount of the API was released in the acidic phase. Despite PVA having gelling properties in aqueous media and the PVA being the major component in the formulation of the filaments and, thus, tablets, the mebeverine hydrochloride was entirely released from this formulation within the first two hours; thus, the test was discontinued. The amount of API released from AQOAT in the acidic phase was independent from the AQOAT grade and was ca. 7%. After transition to the pH = 6.8, sustained release of the API was observed. The drug release from AQOAT AS-LMP and AS-MMP-based tablets have similar courses; over 90% of mebeverine hydrochloride was released after 12 or 15 h, respectively. However, the dissolution from the AQOAT AS-HMP-based formulation is substantially different and it is characterized by markedly extended release; after 24 h, only 52.8 $\pm$ 4.2% of the drug was released. It is caused by the pH-dependent solubility of the polymer. The dissolution of AQOAT AS-HMP occurs at pH levels exceeding 6.5. Given that the dissolution medium has a marginally elevated pH, the pH microenvironment at the polymer-solution interface may significantly impede the dissolution of mebeverine hydrochloride [20]. Moreover, higher acetyl content in AQOAT AS-HMP results in slower drug release due to its increased hydrophobicity and formation of a more robust gel network that controls the drug diffusion rate [21]. The significant delay in the release of the active substance presents an opportunity for further optimization of API release through various modifications to tablet structure, potentially allowing for the customization of the dissolution profile across a broad spectrum. Numerous studies indicate that utilizing 3D-printed tablet designs can effectively modify the release of the active pharmaceutical ingredient to meet specific requirements [22,23].

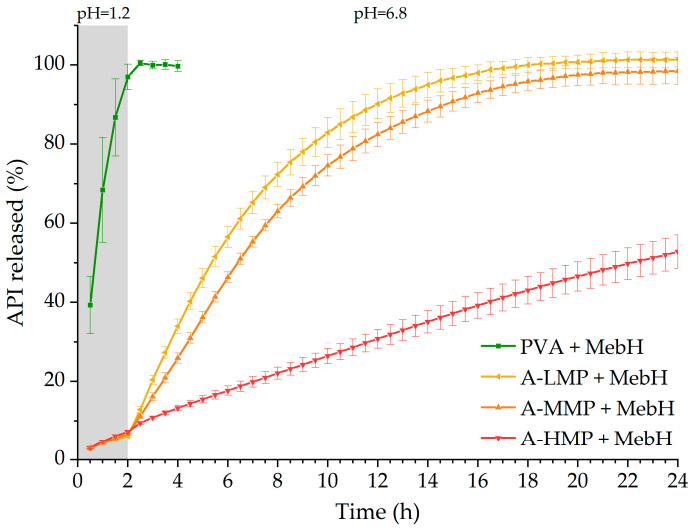


Figure 5. Mebeverine hydrochloride dissolution profiles from 3D-printed tablets.

4. Conclusions

In the presented study, the potential of different grades of hydroxypropylmethylcellulose acetate succinate was evaluated in terms of filament-forming abilities, mechanical properties, printability, and, finally, release modifying abilities. As a comparison, poly(vinyl alcohol) was used. It was found that all tested HPMC-AS grades produced filaments with a uniform diameter but unsatisfactory mechanical properties. Nevertheless, we were able to perform 3D printing by a simple filament procedure to raise the temperature of the filament above its glass transition temperature and, thus, reduce its brittleness and improve printability. The adapter for filament crushing resistance testing, which reflects the forces exerted on the filament in the printhead, which helps to evaluate the printability of the filaments without actual printing process, was developed and tested in this work as well. The release studies showed great potential in sustaining mebeverine hydrochloride release, as it can be prolonged for over 24 h, as in the case of AQOAT AS-HMP. The ability to slow down the release from solid tablets offers great potential for further modification by changing the structure of the tablets through loosening their structure, adding channels, increasing porosity, etc., while still maintaining extended-release characteristics.

Supplementary Materials: The following supporting information can be downloaded at: https://www.mdpi.com/article/10.3390/app16031237/s1, Table S1: raw data from dissolution experiments.

Author Contributions: Conceptualization, M.K. and W.J.; methodology, M.K. and W.J.; validation, M.K., W.J. and M.B.L.N.; investigation, M.K., M.B.L.N., W.J. and J.K.-K.; writing—original draft preparation, M.K. and M.B.L.N.; writing—review and editing, M.K., W.J., J.K.-K., M.P. and A.M.; visualization, M.K. and W.J.; supervision, M.P. and A.M.; project administration, M.K. All authors have read and agreed to the published version of the manuscript.

Funding: The authors would like to acknowledge the financial support of the Erasmus+ Program of the European Union, which enabled the research mobility of Margarida Berardo Lopes Nunes at Chair of Pharmaceutical Technology and Biopharmaceutics, Faculty of Pharmacy, Jagiellonian University Medical College.

Institutional Review Board Statement: Not applicable.

Informed Consent Statement: Not applicable.

Data Availability Statement: The original contributions presented in this study are included in the article/Supplementary Material. Further inquiries can be directed to the corresponding author(s).

Conflicts of Interest: The authors declare no conflicts of interest.

Abbreviations

The following abbreviations are used in this manuscript:

3D	Three-dimensional
API	Active Pharmaceutical Ingredient
DSC	Differential Scanning Calorimetry
FDM	Fused Deposition Modeling
HME	Hot-melt Extrusion
HPMC-AS	Hypromellose Acetate Succinate
MebH	Mebeverine Hydrochloride
ODF	Orodispersible Film
ODT	Orodispersible Tablet
PVA	Poly(vinyl alcohol)
SD	Standard Deviation
T_g	Glass Transition Temperature
YM	Young Modulus

References

1. Couți, N.; Iurian, S.; Porfire, A.; Casian, T.; Iovanov, R.; Tomuță, I. Three-Dimensional Printing in Paediatrics: Innovative Technology for Manufacturing Patient-Centred Drug Delivery Systems. *Pharmaceutics* **2025**, *17*, 1364. [CrossRef]
2. Ahmed, A.A.; Schimmel, K.J.M.; Tubic-Grozdanis, M.; Tuleu, C.; Smith, J.; Soulairol, I.; Dadkhah, A.; Paulson, M.; Lechanteur, A.; Carrez, L.; et al. Expert Opinion on Extrusion-Based Pharmaceutical 3D Printing from the European Society of Hospital Pharmaceutical Technology (GERPAC). *Int. J. Pharm.* **2025**, *686*, 126321. [CrossRef]
3. Elbl, J.; Gajdziok, J.; Kolarczyk, J. 3D Printing of Multilayered Orodispersible Films with In-Process Drying. *Int. J. Pharm.* **2020**, *575*, 118883. [CrossRef] [PubMed]
4. Pyteraf, J.; Jamróz, W.; Kurek, M.; Bąk, U.; Loskot, J.; Kramarczyk, D.; Paluch, M.; Jachowicz, R. Preparation and Advanced Characterization of Highly Drug-Loaded, 3D Printed Orodispersible Tablets Containing Fluconazole. *Int. J. Pharm.* **2023**, *630*, 122444. [CrossRef]
5. Wichniarek, R.; Kuczko, W.; Tomczak, D.; Nowicka, A.; Wojtyłko, M.; Froelich, A.; Osmałek, T. Geometrical Accuracy and Strength of Micro-Needles Made of Polylactide by Fused Filament Fabrication Method. *Adv. Sci. Technol. Res. J.* **2023**, *17*, 116–126. [CrossRef]
6. Oros, D.; Penčić, M.; Orošnjak, M.; Kedziora, S. Additive Manufacturing Technologies and Their Applications in Dentistry: A Systematic Literature Review. *Appl. Sci.* **2025**, *15*, 8346. [CrossRef]
7. Quodbach, J.; Bogdahn, M.; Breitkreutz, J.; Chamberlain, R.; Eggenreich, K.; Elia, A.G.; Gottschalk, N.; Gunkel-Grabole, G.; Hoffmann, L.; Kapote, D.; et al. Quality of FDM 3D Printed Medicines for Pediatrics: Considerations for Formulation Development, Filament Extrusion, Printing Process and Printer Design. *Ther. Innov. Regul. Sci.* **2022**, *56*, 910–928. [CrossRef]
8. Feuerbach, T.; Callau-Mendoza, S.; Thommes, M. Development of Filaments for Fused Deposition Modeling 3D Printing with Medical Grade Poly(Lactic-Co-Glycolic Acid) Copolymers. *Pharm. Dev. Technol.* **2019**, *24*, 487–493. [CrossRef] [PubMed]
9. Korte, C.; Quodbach, J. Formulation Development and Process Analysis of Drug-Loaded Filaments Manufactured via Hot-Melt Extrusion for 3D-Printing of Medicines. *Pharm. Dev. Technol.* **2018**, *23*, 1117–1127. [CrossRef]
10. Oladeji, S.; Mohylyuk, V.; Jones, D.S.; Andrews, G.P. 3D Printing of Pharmaceutical Oral Solid Dosage Forms by Fused Deposition: The Enhancement of Printability Using Plasticised HPMCAS. *Int. J. Pharm.* **2022**, *616*, 121553. [CrossRef]
11. Patil, R.; Bule, P.; Chella, N. Exploration of Conventional and FDM-Mediated 3D Printed Tablets Fabricated Using HME-Based Filaments for pH-Dependent Drug Delivery. *AAPS PharmSciTech* **2025**, *26*, 96. [CrossRef]
12. Goyanes, A.; Fina, F.; Martorana, A.; Sedough, D.; Gaisford, S.; Basit, A.W. Development of Modified Release 3D Printed Tablets (Printlets) with Pharmaceutical Excipients Using Additive Manufacturing. *Int. J. Pharm.* **2017**, *527*, 21–30. [CrossRef]
13. Shojaie, F.; Ferrero, C.; Caraballo, I. Development of 3D-Printed Bicompartmental Devices by Dual-Nozzle Fused Deposition Modeling (FDM) for Colon-Specific Drug Delivery. *Pharmaceutics* **2023**, *15*, 2362. [CrossRef] [PubMed]
14. Dickinson, R.G.; Baker, P.V.; Franklin, M.E.; Hooper, W.D. Facile Hydrolysis of Mebeverine In Vitro and In Vivo: Negligible Circulating Concentrations of the Drug after Oral Administration. *J. Pharm. Sci.* **1991**, *80*, 952–957. [CrossRef] [PubMed]
15. Council of Europe. EDQM—European Directorate for the Quality of Medicines. In *European Pharmacopoeia*, 11th ed.; Council of Europe: Strasbourg, France, 2023.

16. Jamróz, W.; Pyteraf, J.; Kurek, M.; Knapik-Kowalczuk, J.; Szafraniec-Szczęsny, J.; Jurkiewicz, K.; Leszczyński, B.; Wróbel, A.; Paluch, M.; Jachowicz, R. Multivariate Design of 3D Printed Immediate-Release Tablets with Liquid Crystal-Forming Drug—Itraconazole. *Materials* **2020**, *13*, 4961. [CrossRef]
17. Xu, P.; Li, J.; Meda, A.; Osei-Yeboah, F.; Peterson, M.L.; Repka, M.; Zhan, X. Development of a Quantitative Method to Evaluate the Printability of Filaments for Fused Deposition Modeling 3D Printing. *Int. J. Pharm.* **2020**, *588*, 119760. [CrossRef] [PubMed]
18. Dong, F.; Yan, M.; Jin, C.; Li, S. Characterization of Type-II Acetylated Cellulose Nanocrystals with Various Degree of Substitution and Its Compatibility in PLA Films. *Polymers* **2017**, *9*, 346. [CrossRef]
19. Wang, S.-Q.; Cheng, S.; Lin, P.; Li, X. A Phenomenological Molecular Model for Yielding and Brittle-Ductile Transition of Polymer Glasses. *J. Chem. Phys.* **2014**, *141*, 094905. [CrossRef]
20. Bapat, P.; Paul, S.; Thakral, N.K.; Tseng, Y.-C.; Taylor, L.S. Does Media Choice Matter When Evaluating the Performance of Hydroxypropyl Methylcellulose Acetate Succinate-Based Amorphous Solid Dispersions? *Mol. Pharm.* **2023**, *20*, 5714–5727. [CrossRef]
21. Ueda, K.; Higashi, K.; Yamamoto, K.; Moribe, K. Inhibitory Effect of Hydroxypropyl Methylcellulose Acetate Succinate on Drug Recrystallization from a Supersaturated Solution Assessed Using Nuclear Magnetic Resonance Measurements. *Mol. Pharm.* **2013**, *10*, 3801–3811. [CrossRef]
22. Sadia, M.; Arafat, B.; Ahmed, W.; Forbes, R.T.; Alhnan, M.A. Channelled Tablets: An Innovative Approach to Accelerating Drug Release from 3D Printed Tablets. *J. Control. Release* **2018**, *269*, 355–363. [CrossRef] [PubMed]
23. Hu, Z.; Xu, P.; Zhang, J.; Bandari, S.; Repka, M.A. Development of Controlled Release Oral Dosages by Density Gradient Modification via Three-Dimensional (3D) Printing and Hot-Melt Extrusion (HME) Technology. *J. Drug Deliv. Sci. Technol.* **2022**, *71*, 103355. [CrossRef]

Disclaimer/Publisher's Note: The statements, opinions and data contained in all publications are solely those of the individual author(s) and contributor(s) and not of MDPI and/or the editor(s). MDPI and/or the editor(s) disclaim responsibility for any injury to people or property resulting from any ideas, methods, instructions or products referred to in the content.